IOP Conf. Series: Materials Science and Engineering **377** (2018) 012108 doi:10.1088/1757-899X/377/1/012108

Optimisation of hole characteristics in pulsed Nd: YAG laser micro-drilling of AISI 304 stainless steel by Taguchi method

Anita Pritam[1, 3], R R Dash [1], R K Mallik [1], Arun K Parida[2]
[1]Dept. Of mechanical Engineering, CET, Bhubaneswar, Odisha, 751029
[2]Dept. Of mechanical Engineering, GITAM, Bhubaneswar, Odisha

[3]e-mail: anitapritam@gmail.com, ratiranjan.dash@gmail.com

Abstract. The objective of this experimental study is to determine the influence of laser drilling parameters on a flat AISI 304 stainless steel sheet of 1mm thickness with pulsed Nd:YAG laser machining system. Taguchi's L_{25} orthogonal array is used for the experimental design. The machining process parameters such as Lamp current, Pulse frequency, Air pressure and Pulse width are optimized with heat affected zone and hole taper parameters. Grey Relational Analysis (GRA) is used to solve such correlated multi-attribute optimization of drilling operation. The optimal setting parameters for multiple performance characteristics is lamp current at level-1, pulse frequency at level-5, air pressure at level-4 and pulse width at level-5 i.e., $\mathbf{l_1}$-$\mathbf{f_5}$-$\mathbf{p_4}$-$\mathbf{w_5}$. The Analysis of Variance (ANOVA) technique is carried out to check the significance of the models and observed that the lamp current, pulse frequency and air pressure are significant at 95% confidence level. Finally in the confirmation test, it is observed that the grey relational grade is improved from initial process parameter combination.

1. Introduction

The laser micro-drilling process is one of the non-traditional machining process which uses thermal energy to remove material from the work piece surface and hence any complex geometries and difficult to machine materials can be machined easily without any tool-based problem [1, 2]. Due to highly directional, high power density and better focussing characteristics of laser beam; it is useful in processing of several materials. Due to the shorter wavelength (1 μm), and pulse mode, Nd: YAG laser can be absorbed by highly reflective materials which are difficult to machine by CO_2 lasers [3]. Experimental studies on Laser Drilling operations by various researchers show the effect of input process parameters such as laser power, lamp current, pulse frequency, pulse width, pulse number, spot diameter, focal plane position, type and pressure of assist gas, cutting material thickness and its composition, cutting speed, and mode of operation (continuous or pulsed mode) on process performance of interest in Laser drilling operation which are MRR (material removal rate), machined geometry (hole circularity, hole taper, hole diameter, aspect ratio, penetration depth), surface quality (surface morphology, burr deposition rate, spatter), metallurgical characteristics (recast layer, heat affected zone), drilling efficiency and mechanical properties (crack, hardness, strength, etc.).

Due to converging or diverging shape of the laser beam, there always taper exists in laser drilled holes, which can be minimized up to acceptable range [4, 7, 9] by increasing the laser power at constant pulse frequency and the main change in metallurgical characteristics of laser machined parts or work piece is mostly governed by HAZ and recast layer and it is seen that low material thickness and pulse energy gives smaller HAZ [5, 6, 10].

In this work, an experimental investigation has been performed on pulsed Nd: YAG laser micro-drilling of AISI 304 stainless steel. Four independent process parameters, lamp current, pulse frequency, air pressure, and pulse width are considered as input parameters. And the hole taper and HAZ width are considered as the output parameters. The Taguchi method [8] combined with the grey relational analysis [11] is used as a statistical design of the experiment technique to set the optimal process parameters. This optimal result is further verified with ANOVA.

2. Principle of Laser beam drilling

The mechanism of material removal during laser beam drilling consists of three different phases such as (i) melting, (ii) vaporization, and (iii) chemical degradation (chemical bonds are broken which causes the materials to degrade [12, 13]. Being a thermal process, the effectiveness of laser drilling depends on thermal properties and, to a certain extent, the optical properties rather than the mechanical properties of the material to be machined. Block diagram of laser micro drilling showing mechanical mechanism is shown in Figure1.

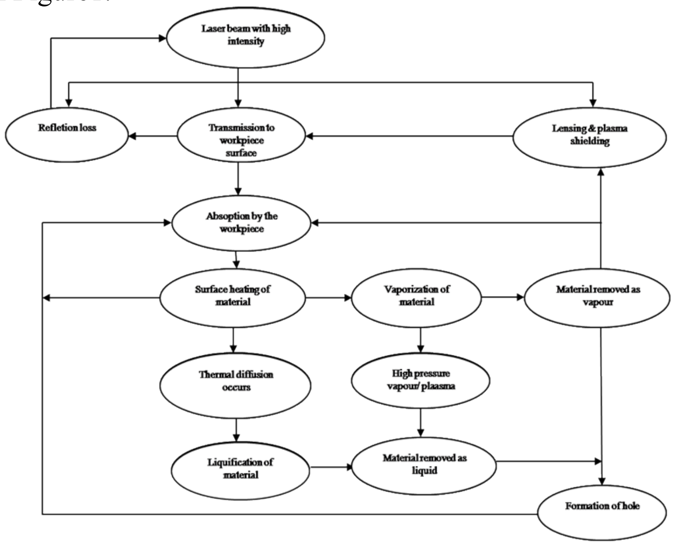

Figure 1. Block diagram of laser micro drilling showing mechanical mechanism

3. Experimental procedure

The experiments were carried out on a flat AISI 304 stainless steel sheet of 1mm thick with composition (C %< 0.08, Si %< 1, Mn%<2, P%<0.045, S%<0.030, Cr% 18-20, Ni% 8-10.6). The work piece thickness was measured by a digital vernier calliper having a least count of 0.001 mm, and is found 1 mm. The work piece was held on the CNC work table using a specially designed fixture.

A 200W pulsed Nd: YAG laser-based CNC machining system, supplied by Suresh Indu-Laser, Pune (India) is used for the experimental study, with subsystems such as power supply unit, the laser source and beam delivery unit, cooling unit, radio frequency Q-switch driver unit, compressed air supply unit, and CNC controllers for X, Y, and Z axes movements. The photographic view of the CNC pulsed Nd: YAG laser machining system is shown in Figure 3.

Taguchi method for four factors at five levels was used for the implementation of orthogonal array experiments. An L_{25} orthogonal array with 25 rows and 4 columns was employed in this work. The experiments were carried out according to the arrangement of the orthogonal array. After the drilling operation, the top and bottom diameters of the micro-holes were measured by an optical measuring microscope (Model SDM-TR-MSU, Sipcon instrument Industries, India) at ×10 magnification. Taper of the drilled hole has been calculated considering the straight taper profile, and the HAZ width had been measured from the top surface only shown in Figure 2 as follows:

$$Taper = \frac{(hole\_dia_{top} - hole\_dia_{bottom})}{2 * thickness} \quad (1)$$

$$HAZ\ width = \frac{(HAZ\_dia_{top} - hole\_dia_{top})}{2} \quad (2)$$

The experimental layout for the laser drilling parameters using the L_{25} orthogonal array and the experimental results and their S/N ratio values are presented in Table 1.

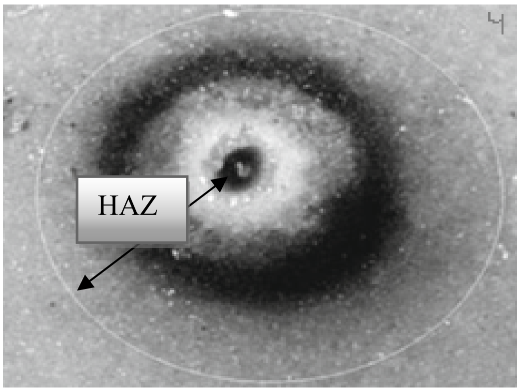

Figure 2. HAZ width of drilled hole from top surface

Figure 3. CNC pulsed Nd: YAG laser M/C system

Table 1 Experimental assignments and results with S/N ratio

Expt. no	Lamp current l(amp) (actual)	Pulse frequency f (kHz) (actual)	Air pressure p(kg/cm2) (actual)	Pulse width w(%) (actual)	HAZ	S/N ratio for HAZ	TAPER	S/N ratio for TAPER
01	16	0.3	0.5	03	0.2608	11.6738	0.0653	23.7017
02	16	1.3	1.0	08	0.1709	15.3452	0.0612	24.2650
03	16	2.3	1.5	13	0.2298	12.7730	0.0613	24.2508
04	16	3.3	2.0	18	0.2041	13.8031	0.0618	24.1802
05	16	4.3	2.5	23	0.0936	20.5745	0.0598	24.4660
06	18	0.3	1.0	13	0.3902	8.1743	0.0598	24.4660
07	18	1.3	1.5	18	0.3702	8.6313	0.0331	29.6034
08	18	2.3	2.0	23	0.2560	11.8352	0.0497	26.0729
09	18	3.3	2.5	03	0.2782	11.1129	0.0601	24.4225
10	18	4.3	0.5	08	0.2315	12.7090	0.0678	23.3754
11	20	0.3	1.5	23	0.3408	9.3500	0.0529	25.5309
12	20	1.3	2.0	03	0.3319	9.5799	0.0424	27.4527
13	20	2.3	2.5	08	0.2989	10.4895	0.0542	25.3200
14	20	3.3	0.5	13	0.3302	9.6245	0.0798	21.9599
15	20	4.3	1.0	18	0.2618	11.6406	0.0783	22.1248
16	22	0.3	2.0	08	0.4912	6.1748	0.0761	22.3723
17	22	1.3	2.5	13	0.4986	6.0450	0.0785	22.1026
18	22	2.3	0.5	18	0.6724	3.4474	0.1052	19.5597
19	22	3.3	1.0	23	0.3986	7.9893	0.1189	18.4964
20	22	4.3	1.5	03	0.4014	7.9285	0.1068	19.4286
21	24	0.3	2.5	18	0.4803	6.3697	0.0812	21.8089
22	24	1.3	0.5	23	0.4269	7.3935	0.0689	23.2356
23	24	2.3	1.0	03	0.4987	6.0432	0.0916	20.7621
24	24	3.3	1.5	08	0.3412	9.3398	0.1021	19.8195
25	24	4.3	2.0	13	0.3221	9.8402	0.0773	22.2364

4. Optimization of individual performance characteristics

4.1 Determination of optimal process parameters for HAZ and Taper

In this section, L_{25} orthogonal array is used to determine the optimal process parameters. Machining results are reported in using S/N ratio and ANOVA analysis by using statistical software MINITAB-14. In Taguchi there are three performance characteristics such as higher-is-better, nominal-is-better and lower-is-better. Here lower-is-better is used to find the optimal process parameter for HAZ and Taper.

4.2 Analysis of S/N ratio for HAZ

As the experimental design is orthogonal, so it is possible to separate out the effect of each process parameter at different levels. From the response Table 2 of mean S/N ratio for HAZ, it is observed that current is the most effective parameter followed by frequency and pulse width. It is also observed that air pressure has least effect on HAZ.

Table 2 Response table of mean S/N ratio for HAZ

Symbol	Process parameters	Mean S/N ratio						Rank
		Level-1	Level-2	Level-3	Level-4	Level-5	Max-Min	
l	Current	14.834	10.493	10.137	6.317	7.797	8.517	1
f	Frequency	8.349	9.399	8.918	10.374	12.539	4.190	2
p	Pressure	8.970	9.838	9.605	10.247	10.918	1.949	4
w	Width	9.268	10.812	9.291	8.778	11.428	2.650	3
		Total mean S/N ratio = 9.92dB						

From main effects plot for SN ratio (Figure 4), the optimal process parameters for HAZ are obtained such as lamp current at level-1, pulse frequency at level-5, air pressure at level-5 and pulse width at level-5 i.e., $\mathbf{I_1}$-$\mathbf{f_5}$-$\mathbf{p_5}$-$\mathbf{w_5}$.

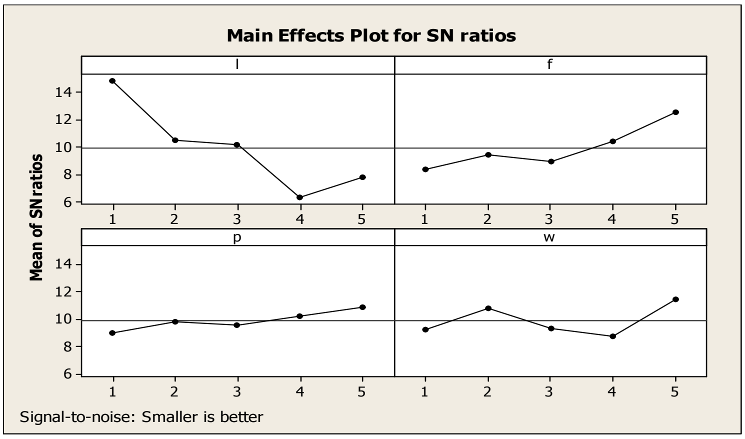

Figure 4. Mean S/N graph for HAZ

4.3. ANOVA for HAZ

The purpose of the ANOVA is to find the statistical significance of process parameters on the response shown in Table 3 and it is observed that the lamp current, pulse frequency and pulse width are with a P value less than 0.05 that means these are significant at 95% confidence level.

Table 3 ANOVA table for HAZ

Source	DF	SS	MS	F	P
l	4	0.262720	0.065680	54.77	0.000
f	4	0.063355	0.015839	13.21	0.001
p	4	0.012019	0.003005	2.51	0.125
w	4	0.030746	0.007687	6.41	0.013
Error	8	0.009593	0.001199		
Total	24	0.378434			

R-Sq = 97.47% R-Sq (adj) = 92.40%

4.4. Analysis of S/N ratio for Taper

Similarly the S/N ratio for Taper is calculated. Here lower-is-better is used to find the optimal process parameter for Taper. From response Table 4, it is observed that the current is again the most effective parameter for Hole taper followed by pulse frequency and air pressure. From the mean S/N ratio for Taper, the optimal process parameters are obtained such as lamp current at level-2, pulse frequency at level-2, air pressure at level-4 and pulse width at level-5 i.e., $\mathbf{I_2\text{-}f_2\text{-}p_4\text{-}w_5}$. And the result is shown in Figure 5.

Table 4 Response table of mean S/N ratio for Taper

Symbol	Process parameters	Mean S/N ratio						Rank
		Level-1	Level-2	Level-3	Level-4	Level-5	Max-Min	
I	Current	24.17	25.59	24.48	20.39	21.57	5.20	1
f	Frequency	23.58	25.33	23.19	21.78	22.33	3.56	2
p	Pressure	22.37	22.02	23.73	24.46	23.62	2.44	3
w	Width	23.15	23.03	23.00	23.46	23.56	0.56	4
		Total mean S/N ratio = 23.24 dB						

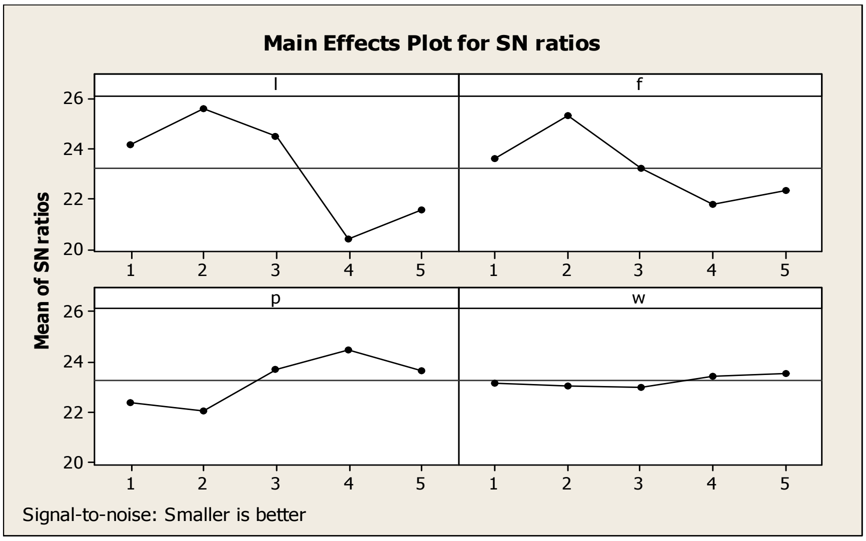

Figure 5. Mean S/N graph for Taper

4.5. ANOVA for Taper

From ANOVA analysis shown in Table 5, it is clearly found that lamp current, pulse frequency and air pressure with a P value less than 0.05 that means these are significant at 95% confidence level.

Table 5 ANOVA table for Taper

Source	DF	SS	MS	F	P
I	4	0.0065586	0.0016396	40.20	0.000
f	4	0.0022398	0.0005600	13.73	0.001
p	4	0.0013360	0.0003340	8.19	0.006
w	4	0.0000281	0.0000070	0.17	0.947
Error	8	0.0003263	0.0000408		
Total	24	0.0104889			

R-Sq = 96.89% R-Sq (adj) = 90.67%

5. Grey relation analysis

In the grey relational analysis, the experimental results are first normalized in the range between zero and unity. This process of normalization is known as the grey relational generation. After then the grey relational coefficient is calculated from the normalized experimental data to express the relationship between the desired and actual experimental data. Then, the overall grey relational grade is calculated by averaging the grey relational coefficient corresponding to each selected process response. The overall evaluation of the multiple process responses are based on the grey relational grade. This method converts a multiple response process optimization problem with the objective function of overall grey relational grade. The corresponding level of parametric combination with highest grey relational grade is considered as the optimum process parameter.

5.1 Determination of optimal process parameters for Grey relational grade

The higher grey relational grade implies that the corresponding parameter combination is closer to the optimal. Thus the grey relational grade with S/N ratio is found out which is shown in Table 6.

The optimal process parameters are obtained from the response graph as shown in Figure 6. The optimal setting parameters for multiple performance characteristics is lamp current at level-1, pulse frequency at level-5, air pressure at level-4 and pulse width at level-5 i.e., $\mathbf{I_1\text{-}f_5\text{-}p_4\text{-}w_5}$.

Table 6 Grey relational grade table

Expt. No	Responses		Grey relational generation		Evaluation of Δ_{oi}		Grey relational coefficient(ψ=0.5)		Grey relational grade	S/N ratio
	HAZ	Taper	HAZ	Taper	HAZ	Taper	HAZ	Taper		
01	0.2608	0.0653	0.820738	0.624709	0.179262	0.375291	0.736093	0.571238	0.653666	-3.69289
02	0.1709	0.0612	1	0.672494	0	0.327506	1	0.604225	0.802113	-1.91529
03	0.2298	0.0613	0.882552	0.671329	0.117448	0.328671	0.809785	0.603376	0.70658	-3.01677
04	0.2041	0.0618	0.933799	0.665501	0.066201	0.334499	0.883078	0.599162	0.74112	-2.60223
05	0.0936	0.0598	1.154138	0.688811	-0.15414	0.311189	1.445662	0.616379	1.03102	0.26535
06	0.3902	0.0598	0.562712	0.688811	0.437288	0.311189	0.533454	0.616379	0.574917	-4.80790
07	0.3702	0.0331	0.602592	1	0.397408	0	0.55716	1	0.77858	-2.17393
08	0.256	0.0497	0.830309	0.806527	0.169691	0.193473	0.746613	0.721008	0.733811	-2.68832
09	0.2782	0.0601	0.786042	0.685315	0.213958	0.314685	0.700321	0.613734	0.657028	-3.64833
10	0.2315	0.0678	0.879163	0.595571	0.120837	0.404429	0.805364	0.552835	0.679099	-3.36133
11	0.3408	0.0529	0.661216	0.769231	0.338784	0.230769	0.596101	0.684211	0.640156	-3.87428
12	0.3319	0.0424	0.678963	0.891608	0.321037	0.108392	0.608986	0.821839	0.715413	-2.90887
13	0.2989	0.0542	0.744766	0.754079	0.255234	0.245921	0.662046	0.670313	0.666179	-3.52818
14	0.3302	0.0798	0.682353	0.455711	0.317647	0.544289	0.611511	0.478795	0.545153	-5.26964
15	0.2618	0.0783	0.818744	0.473193	0.181256	0.526807	0.733938	0.486947	0.610442	-4.28711
16	0.4912	0.0761	0.361316	0.498834	0.638684	0.501166	0.439103	0.499418	0.469261	-6.57172
17	0.4986	0.0785	0.34656	0.470862	0.65344	0.529138	0.433486	0.485844	0.459665	-6.75117
18	0.6724	0.1052	0	0.159674	1	0.840326	0.333333	0.373043	0.353188	-9.03987
19	0.3986	0.1189	0.545962	0	0.454038	1	0.524088	0.333333	0.428711	-7.35671
20	0.4014	0.1068	0.540379	0.141026	0.459621	0.858974	0.521039	0.367925	0.444482	-7.04292
21	0.4803	0.0812	0.383051	0.439394	0.616949	0.560606	0.447648	0.471429	0.459538	-6.75357
22	0.4269	0.0689	0.489531	0.582751	0.510469	0.417249	0.49482	0.545108	0.519964	-5.68054
23	0.4987	0.0916	0.346361	0.318182	0.653639	0.681818	0.433411	0.423077	0.428244	-7.36617
24	0.3412	0.1021	0.660419	0.195804	0.339581	0.804196	0.595535	0.383378	0.489456	-6.20572
25	0.3221	0.0773	0.698504	0.484848	0.301496	0.515152	0.623834	0.492537	0.558186	-5.06443

5.2. ANOVA for Grey relational grade

From the Table 7, it is clearly found that lamp current, pulse frequency and air pressure with a P value less than 0.05 that means these are significant at 95% confidence level.

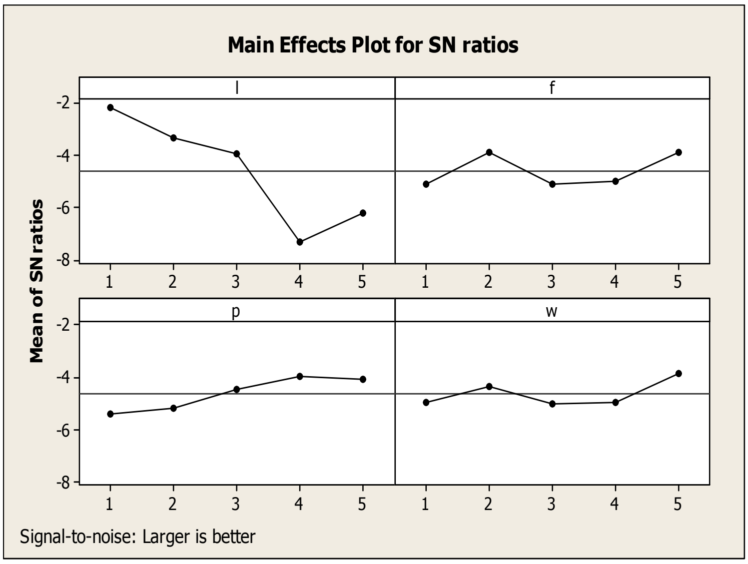

Figure 6 Grey relational grade graphs of multiple performance characteristics

Table 7 ANOVA for grey relational grade

Source	DF	SS	MS	F	P
l	4	0.417977	0.104494	42.05	0.000
f	4	0.049794	0.012449	5.01	0.026
p	4	0.041523	0.010381	4.18	0.041
w	4	0.033951	0.008488	3.42	0.066
Error	8	0.019882	0.002485		
Total	24	0.417977			

R-Sq = 96.47% R-Sq (adj) = 89.41%

5.3. Confirmation test for Grey relational grade

After the optimum level of machining parameters in multiple performance characteristics identified, a verification test needs to be carried out in order to check the accuracy of the analysis. Table 8 shows the comparison of estimated grey relational grade with the actual grey relational grade obtained in experiment using the optimal drilling parameters.

Table 8 Results for the confirmation tests

	Initial process parameter	Optimal process parameter	
		Prediction	experiment
Level	I_5-f_4-p_3-w_2	I_1-f_5-p_4-w_5	I_1-f_5-p_4-w_5
HAZ	0.3412		0.1686
Taper	0.1021		0.0587
Grey relational Grade	0.48946	-0.0833638	0.832505
Improvement of Grey relational Grade= 0.35			

It is also found that the improvement of grey relational grade from initial process parameter combination to the optimal process parameter combination is 0.35.

6. Conclusions

The laser micro-drilling operation on AISI 304 stainless steel was performed using pulsed Nd: YAG laser machining system. The optimal process parameters (lamp current, pulse frequency, air pressure and pulse width) combination on both HAZ and Hole Taper has been determined by a multi response optimization technique. The use of the Taguchi orthogonal array with grey relational analysis to

IOP Conf. Series: Materials Science and Engineering **377** (2018) 012108 doi:10.1088/1757-899X/377/1/012108

optimize the machining process with the multiple performance characteristics is used in this work. The grey relational grade, which is a grey relational analysis of the experimental results of HAZ and taper, is used for conversion of single performance characteristics optimization and the improvement of grey relational grade from initial process parameter combination to the optimal process parameter combination is 0.35. As a result, optimization of the complicated multiple performance characteristics was simplified through this approach. It is shown that the performance characteristic of the machining process such as HAZ and Taper are improved together by using this approach.

Reference

[1] Gillner, A.; Holtkamp, J.; Hartmann, C.; Olowinsky, A.; Gedicke, J.; Klages, K.; Bosse, L.; Bayer, A.: Laser Applications in microtechnology. J. Mater. Process. Technol. **167**, 494–498 (2005)

[2] T. Norikazu, Y. Shigenori, H. Masao, Present and future of lasers for fine cutting of metal plate, Journal of Materials Processing Technology 62 (1996) 309–314.

[3] J. Meijer, Laser beam machining (LBM), state of the art and new opportunities, Journal of Materials Processing Technology 149 (2004) 2–17.

[4] R. Biswas, A.S.Kuar , S.Sarkar , S.Mitra, A parametric study of pulsed Nd:YAG laser micro-drilling of gamma-titanium aluminide, Optics & Laser Technology 42 (2010) 23–31.

[5] H.K. Sezer, L. Li, M. Schmidt, A.J. Pinkerton, B. Anderson, P. Williams, Effect of beam angle on HAZ, recast and oxide layer characteristics in laser drilling of TBC nickel superalloys, International Journal of Machine Tools and Manufacture 46 (15) (2006) 1972–1982.

[6] Sumanta Panda , Debadutta Mishra , Bibhuti B. Biswal, Determination of optimum parameters with multi-performance characteristics in laser drilling-A grey relational analysis approach, Int J Adv Manuf Technol (2011) 54:957–967.

[7] Carlo Alberto Biffi, Nora Lecis, Barbara Previtali, Maurizio Vedani, Gian Marco Vimercati, Fiber laser microdrilling of titanium and its effect on material microstructure, Int J Adv Manuf Technol (2011) 54:149–160.

[8] Timur Canel, A.Ugur Kaya,Bekir Celik, Parameter optimization of nanosecond laser for microdrilling on PVC by Taguchi method, Optics & Laser Technology 44 (2012) 2347–2353.

[9] A. Bharatish, H. N. Narasimha Murthy, B. Anand, C. D. Madhusoodana, G.S. Praveena, M.Krishna, Characterization of hole circularity and heat affected zone in pulsed CO_2 laser drilling of alumina ceramics, Optics & Laser Technology 53 (2013) 22–32.

[10] S. Bandyopadhyay, J.K.S. Sundar, G. Sundarrajan, S.V. Joshi, Geometrical features and metallurgical characteristics of Nd:YAG laser drilled holes in thick IN718 and Ti–6Al–4V sheets, Journal of Materials Processing Technology 127 (2002) 83–95.

[11] D. Ganguly, B. Acherjee, A.S. Kaur, S. Mitra, Hole characteristics optimization in Nd:YAG laser Micro-drilling of zirconium oxide by grey relation analysis, Int J Adv Manuf Technol (2012) 61:1255-1262.

[12] J.K.S. Sundar, S.V. Joshi, Laser cutting of materials, Centre for Laser Processing of Materials, International Advance Research Centre for Powder Metallurgy and New Materials, Hyderabad.

[13] D.T. Pham, S.S. Dimov, P.T. Petkov, Laser milling of ceramic components, International Journal of Machine Tools and Manufacture 47 (2007) 618–626.